Non-chemical approach toward 2D self-assemblies of Ag nanoparticles via cold plasma treatment of substrates

2011 Nanotechnology 22 275601

(http://iopscience.iop.org/0957-4484/22/27/275601)

Nanotechnology **22** (2011) 275601 (7pp) doi:10.1088/0957-4484/22/27/275601

Non-chemical approach toward 2D self-assemblies of Ag nanoparticles via cold plasma treatment of substrates

Karolina Siskova[1,4], Klara Safarova[1], Jung Hwa Seo[2,5], Radek Zboril[1] and Miroslav Mashlan[3]

[1] Regional Centre of Advanced Technologies and Materials, Department of Physical Chemistry, Faculty of Science, University of Palacky, Slechtitelu 11, 78371 Olomouc, Czech Republic
[2] Center for Polymers and Organic Solids and Department of Chemistry and Biochemistry, University of California, Santa Barbara, CA 93106, USA
[3] Regional Centre of Advanced Technologies and Materials, Department of Experimental Physics, Faculty of Science, University of Palacky, Slechtitelu 11, 78371 Olomouc, Czech Republic

E-mail: karolina.siskova@upol.cz

Received 14 January 2011, in final form 18 March 2011
Published 20 May 2011
Online at stacks.iop.org/Nano/22/275601

Abstract
The nano-modification of selected substrates by means of atmospheric cold plasma treatment was exploited for the two-dimensional (2D) self-assembling of silver nanoparticles (Ag NPs). Such a useful combination of the cold plasma treatment of substrate surface and an immediate easy deposition of Ag NPs creating the 2D self-assemblies on the substrates is published for the first time, to the best of our knowledge. Except for the cold plasma treatment, mainly the following parameters influenced the resulting NP assemblies: the choice of solvent mixture, concentration of Ag NP dispersions, and the deposition technique. The 2D self-assemblies of Ag NPs, providing the same work function as a Ag electrode, were formed on the cold plasma-treated substrates when a drop-casting technique was employed. The possibility of an easy preparation of the Ag NP 2D self-assemblies on substrates without using any chemical agents and/or evaporating chamber could be exploited, e.g. in photovoltaic and light-emitting diode devices.

(Some figures in this article are in colour only in the electronic version)

1. Introduction

Silver nanoparticles (NPs) have gained substantial attention due to their unique optical, electrical [1], and antimicrobial properties [2]. Among other features, surface plasmons (i.e. the collective oscillations of free electrons) and the high electric conductivity of NPs can be successfully exploited in organic solar cells (OSC) and organic light-emitting diode (OLED) devices as evidenced for instance in [3–6]. Markedly enhanced efficiencies of OLED and OSC devices were reached due to the presence of noble metal NPs in their structures, namely when 2D arrays of Ag NPs were placed on an ITO electrode (i.e. optically transparent substrate covered by a conductive layer of indium–tin-oxide) [3–5]. The deposition of NPs on substrates can be achieved using several approaches: (i) thermal evaporation [3, 4]; (ii) pulse-current electro-deposition [5]; (iii) using the layer-by-layer technique [6]; (iv) using lithography [7]; and (v) via chemical bonds [8]. Another possibility is (vi) to cover nanoparticles by a suitable coating consisting of organic molecules [9]. Several kinds of directed self-assembly of nanoparticles have been recently summarized and critically discussed in a review article by Grzelczak *et al* [10]. At this point, it should be remembered that the processes of chemical treatment, (v) and (vi), can be

[4] Author to whom any correspondence should be addressed.
[5] Present address: Department of Materials Physics, College of Natural Science, Dong-A University, 840 Hadan2dong, Sahagu, Busan, 604-714, Korea.

environmentally unfriendly, expensive, and the resulting NP assemblies possess substantially different optical and electrical properties than pure NPs. On the other hand, the above-mentioned techniques (i) and (ii) require high vacuum and/or current. Regarding all these aspects and with respect to the desired NPs self-assembling on transparent substrates used in OSC and/or OLED, a non-chemical approach, without using high vacuum or temperature, has to be chosen for potential industrial applications.

Except for the introduction of noble metal NPs into functional opto-electronic devices, a plasma treatment of ITO-coated substrates turned out to be another very efficient tool for a significant improvement of OLED performance [11, 12]. Plasma is a quasineutral (i.e. numbers of positive and negative charges are equal) mixture containing electrons, ions, photons, neutral, and excited species (including vibrationally, rotationally, and translationally excited species). According to energy levels, plasmas can be classified as high- and low-temperature ones [13]. The term low-temperature plasma includes thermal and non-thermal plasmas, the latter usually referred to as cold plasmas. Based on the mechanism of cold plasma generation, applied atmosphere, and electrode geometry, many types of cold plasmas can be distinguished. From this point on we will focus on a particular type of cold plasma: atmospheric dielectric-barrier discharge (DBD). The principles as well as the main industrial applications of DBD have been nicely summarized in Kogelschatz's review [14]. Surface modifications induced by DBD treatment have been investigated in the cases of polymers [15–17], textile fibers [18–20], membranes [21], adsorbents [22], and electrodes [11, 12, 23–25].

In the opto-electronic devices, the work function of conductive substrates plays a crucial role for the charge injection and charge collection which has been clearly explained in the literature [26–28]. In general, the better the energy-level alignment at the electrode/organic interface, the more efficient the charge transport and, thus, the more efficient the opto-electronic device that can be obtained. Therefore, when 2D assemblies of NPs on transparent electrodes are achieved, the work function of NP-modified electrodes has to be determined so that they can be considered as applicable for a particular opto-electronic device.

In this paper, we have developed the process of a non-chemical deposition of Ag NPs onto clean substrates which were pre-treated by the cold plasma. The cold plasma treatment is realized by means of a diffuse coplanar surface barrier discharge generator (DCSBD) under ambient conditions (in the air, at room temperature and atmospheric pressure). Subsequently, Ag NPs have been deposited by two different deposition techniques. As far as we know, nobody has yet published research on the usage of the cold plasma treatment for NP assembling. Moreover, we have determined the work function of substrates which have been and have not been modified by Ag NPs using ultraviolet photoelectron spectroscopy (UPS). Further instrumentation which has been used includes x-ray photoelectron spectroscopy (XPS), UV–visible (UV–vis) absorption spectroscopy, dynamic light scattering (DLS), zeta-potential measurements, energy dispersive x-ray spectrometry (EDX), transmission electron microscopy (TEM), scanning electron microscopy (SEM), and atomic force microscopy (AFM).

2. Materials and methods

2.1. Materials

Pieces of microscopic glass, 100 nm-ITO-coated glass purchased from Solemns (30–50 Ω) and/or 100 nm-ITO-coated polyester (PET) foils purchased from Sigma-Aldrich (60 Ω/sq) were carefully cleaned by using isopropylalcohol (Lach-Ner Ltd, p.a) and then dried by purging nitrogen flow. The Ag NPs stock-solution was prepared by a reduction method using maltose as previously described elsewhere [29]. Ag NPs in the stock-solution were characterized by means of UV–visible absorption, DLS, zeta-potential measurements, and TEM. The diluted Ag NP solutions which were further used for experiments, were prepared as follows: 5 ml of the Ag NP stock-solution mixed together with either ultrapure water (Millipore, 18 MΩ cm) and/or ethanol (99.8%, for UV spectroscopy, Lach-Ner) to the final volume of 10 ml.

2.2. Instrumentation

The DCSBD (diffuse coplanar surface barrier discharge) generator consists of 38 parallel stripline silver electrodes embedded 0.5 mm below the surface of 96% Al_2O_3 ceramics. 14 kHz supplied by a high-voltage generator creates the cold plasma in the vicinity of the ceramic surface (up to a height of 0.5 mm above the ceramic surface). The plasma is generated in a rectangle of dimensions 200 × 80 mm^2 which consists of 38 parallel (along the long edge) plasma-active lines. The activation of substrates was performed by 2 min cold plasma treatment at room temperature in air. UV–vis spectra of the Ag NP solutions were recorded on a Specord S600 (Analytic Jena). DLS and zeta potentials were measured on a Zetasizer Nano Series (Malvern Instruments), which enables us to determine zeta potentials in aqueous and non-aqueous dispersions using patented M3-PALS (phase analysis light scattering) technology. Morphological study was done on a JEOL JEM-2010 transmission electron microscope equipped with a LaB_6 cathode (accelerating voltage of 160 kV; a point-to-point resolution of 0.194 nm). A drop of the Ag NP stock-solution was placed onto a holey-carbon film supported by a copper TEM grid and air-dried at room temperature. AFM topographic images of ITO-coated substrates were recorded on a Ntegra microscope in non-contact mode. SEM images of ITO-coated substrates were measured on a Hitachi SU 6600 microscope working at 7 kV and/or 10 kV prior to and after their cold plasma treatment and modification by Ag NPs. Ag presence was proven by EDX measurements, but the quantitative analysis was performed by XPS. The UPS and XPS analysis chamber was equipped with a hemispherical electron energy analyzer (Kratos Ultra Spectrometer) and maintained at 1×10^{-9} Torr. The UPS measurements were carried out using the He I ($h\nu = 21.2$ eV) source, while XPS was measured using monochromatized Al Kα ($h\nu = 1486.6$ eV) excitation. The electron energy analyzer was

Table 1. Zeta potentials of stock and diluted Ag NP dispersions employed for further experiments.

Concentration (mg l^{-1})	Sample	Zeta potential (mV)	Standard deviation (mV)
160	Ag NPs stock-solution	−35.3	0.9
80	5 ml Ag NPs stock-sol. + 5 ml H_2O	−30.7	0.3
80	5 ml Ag NPs stock-sol. + 5 ml EtOH	−9.8	1.2

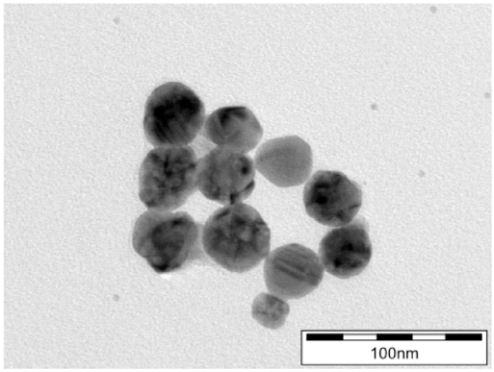

Figure 1. TEM image of Ag NPs which have been employed in the experiments.

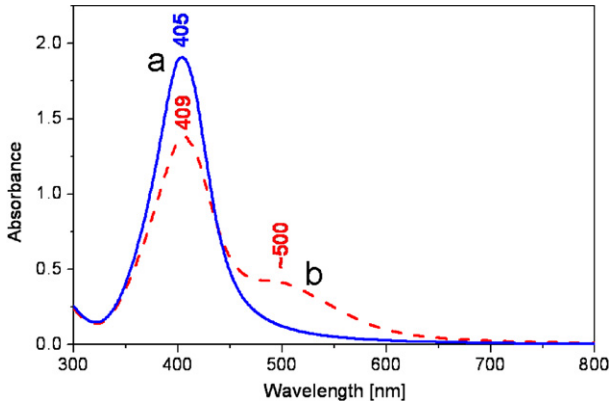

Figure 2. UV–vis absorption spectra of (a) Ag NPs dispersed in ultrapure water (80 mg Ag/l) and (b) Ag NPs dispersed in ethanol/water (1/1, v/v) solution (80 mg Ag/l).

operated at a constant pass energy of 10 eV (for UPS) and at 40 eV (for HR-XPS). During UPS measurements, a sample bias of −9 V was used in order to separate the sample and the secondary edge for the analyzer.

3. Results and discussion

3.1. Characterization of Ag NPs solutions

The as-prepared Ag NPs stock-solution was characterized by means of TEM, DLS, zeta potential, and after an appropriate dilution (by ultrapure water) by UV–vis absorption spectroscopy. TEM images showed Ag NPs of sizes 31 ± 4 nm in diameter (figure 1). DLS measurements revealed sizes at around 34 ± 3 nm in diameter. Both values are in good agreement since the hydrodynamic diameter is measured by DLS, i.e. a silver NP together with its electric bi-layer in a solution; while only the metallic part of Ag NPs is visualized by TEM images. Therefore, smaller size values can be obtained by TEM than by DLS measurements. The sizes of Ag NPs in tens of nanometers were implicitly confirmed by UV–vis absorption spectroscopy as well because the diluted Ag NPs stock-solution provided a distinct surface plasmon band in the visible region with the maximum located at around 405 nm (figure 2, curve (a)). It should be noted that the position of the Ag NP surface plasmon maximum is influence not only by NP size, but also by the NP shape, dielectric constant of NP surroundings, interaction between NPs, and the aggregation state of NPs. In the next step, we prepared two different Ag NP solutions from the Ag NPs stock-solution by a particular dilution using ultrapure water or ethanol (details are provided in the experimental section). We characterized the diluted Ag NP solutions by UV–vis absorption and zeta-potential measurements (figure 2 and table 1). While the aqueous solutions manifested themselves by the position of the absorption maximum at 405 nm (curve (a) in figure 2); the Ag NPs in ethanol/water mixtures revealed two overlapping bands with significant red-shifts (curve (b) in figure 2). Under the assumption that any dissolution of Ag NPs and consequent Ostwald ripening[6] did not proceed, the size and shape of Ag NPs in the solutions remained the same as in the stock-solution. Therefore, the observed changes in the absorption spectra of Ag NPs in ethanol/water mixtures were induced by the changes in the NPs' interactions, changes in dielectric constant of the NPs' surroundings and, as a consequence, by NP aggregation. The stability of Ag NPs against aggregation can be evaluated by measuring zeta potentials of the NP solutions. The stock-solution and diluted aqueous Ag NP solutions revealed zeta potentials at around −30 mV, i.e. a typical value for non-aggregating NPs. On the contrary, the average value of Ag NPs zeta potential in the ethanol/water mixture was rather low in absolute value (table 1). Obviously, the aggregation of Ag NPs in the ethanol/water solution took place due to a decreased electrostatic repulsion between Ag NPs. The extent of Ag NP aggregation followed by UV–vis absorption spectroscopy remained the same in the range of 1 h, however, it continued in the range of days (not shown here). For our further experiments, the diluted Ag NP solutions were always employed within several minutes after their preparation in order to prevent the aggregation of Ag NPs in the ethanol/water mixture and thus to avoid the introduction of an uncontrollable parameter.

[6] This ripening process involves 'the growth of larger crystals from those of smaller size which have a higher solubility than the larger ones' [30].

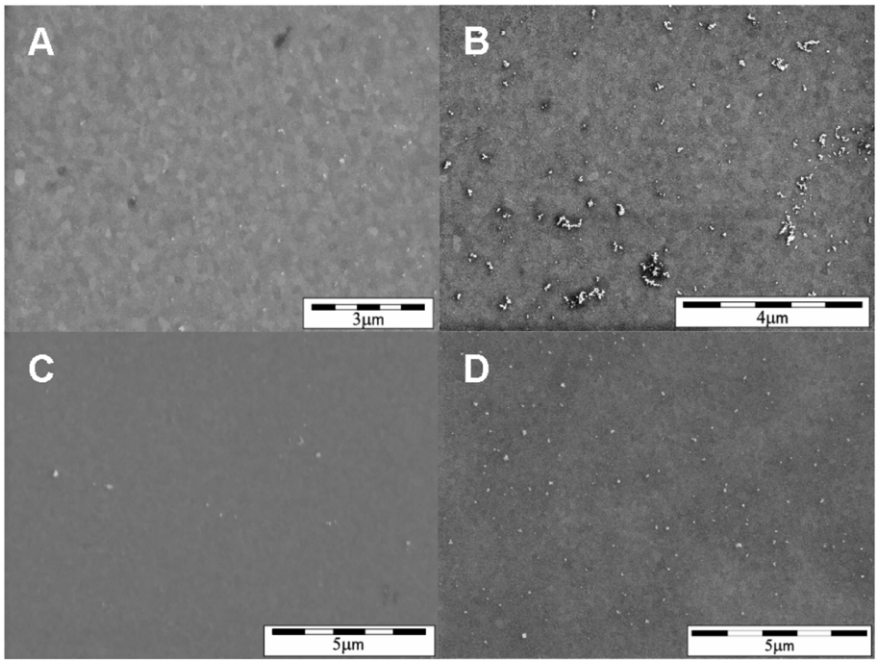

Figure 3. SEM images of untreated ((A), (C)) and cold plasma-treated ((B), (D)) ITO-coated substrates immersed into the diluted Ag NP aqueous solutions ((A), (B)) and ethanol/water (1/1, v/v) solution ((C), (D)) for 2 min.

3.2. Effect of cold plasma treatment of substrates on degree of Ag NP coverage

Since it is known that the plasma-activation works for a limited time period only (usually 1–2 min) [13], cleaned plasma-treated substrates were immersed for 2 min into the diluted Ag NP solutions immediately after their cold plasma treatment. The cold plasma-untreated substrates immersed into the Ag NP solutions for the same time period served as references. The SEM images in figure 3 give evidence about the positive effect of the cold plasma treatment on the degree of Ag NPs coverage of ITO-coated substrates. A rather higher number of Ag NPs on the plasma-treated, figures 3(B) and (D), than on the untreated ITO substrates, figures 3(A) and (C), is clearly distinguished. It can thus be concluded that the Ag NPs dispersed in water and/or in ethanol/water mixtures preferentially interact with the cold plasma-treated substrates. (At this point, it should be mentioned that only the conductive substrates could be visualized and investigated by means of SEM techniques. AFM has been used for the two other types of substrates under investigation.)

There are two possible reasons for the improved interaction between Ag NPs and ITO surfaces induced by the cold plasma treatment: (a) physical and (b) chemical ones. Considering the former, the ITO surface is roughened by the plasma treatment and, consequently, more Ag NPs are captured from their dispersions. However, no significant roughening was confirmed by AFM measurements: the ITO surface roughness determined prior to and after the cold plasma treatment was approximately the same (1.46 nm and 1.51 nm, respectively, over a 2×2 μm^2 surface area). Considering the chemical reason, we performed XPS measurements on the plasma-treated and -untreated ITO substrates. The results are presented in table 2. Obviously, a higher content of oxygen and, simultaneously, a lower content of carbon have been detected in the plasma-treated ITO substrates (table 2). This is in good agreement with the literature [11, 12]. The higher amount of oxygen can be related to an increased hydrophilicity as evidenced in [15–17, 21, 25] for instance. Therefore, an increased surface hydrophilicity of the plasma-treated ITO surfaces can be assumed in our case as well. This consequently leads to a higher volume of the diluted Ag NP solutions remaining on ITO surfaces when the ITO-coated substrates are removed from the Ag NP dispersions and allowed to dry in air. The higher volume of remaining Ag NP solutions implies a higher number of dispersed Ag NPs and, consequently, more Ag NPs encountered on the cold plasma-treated versus untreated ITO-coated substrates, i.e. exactly the results observed in figure 3.

Table 2. Compositions in atomic per cent (at.%) derived from XPS.

Sample	C 1s (at.%)	O 1s (at.%)
Bare ITO	75.4	24.6
Plasma-treated ITO	61.4	38.6

3.3. Effect of solvent evaporation rate on coverage character of plasma-treated substrates by Ag NPs

Comparing figures 3(B) and (D), which represent the characteristic SEM images of the particular NP-modified plasma-treated ITO surfaces, large aggregates of Ag NPs on the ITO surface can be seen in the case where the substrates were immersed into the diluted aqueous Ag NP solutions, figure 3(B). Surprisingly, randomly dispersed Ag NPs and/or

relatively small compact aggregates of NPs on the ITO surface can be seen in figure 3(D) (i.e. when ITO is immersed into the Ag NPs in ethanol/water mixtures). Based solely on the UV–vis absorption measurements of the diluted Ag NP solutions (figure 2), quite opposite results could be expected, i.e. NP aggregates on the ITO substrate immersed in the ethanol/water mixtures. Except for the solvent, all the other parameters were held the same. Therefore, it can be hypothesized that ethanol is the key factor inducing the observed differences in the character of the ITO coverage by Ag NPs.

The unexpected result can be explained by different rates of solvent evaporation under ambient conditions (i.e. at atmospheric pressure and room temperature). Indeed, there are significant differences in the evaporation rate of a drop containing purely water and another one consisting of an ethanol/water mixture. Similar behavior of the NPs self-assembling dependent on the dynamics of the evaporating solvent has been observed and theoretically simulated in [31]. We can thus conclude that the slower the evaporation rate of a solvent, the longer time provided to the NP aggregation. Hence, larger NP aggregates were observed on the ITO surfaces when the diluted aqueous Ag NP solutions used, figure 3(B). A few small compact aggregates of NPs distinguishable in figure 3(D) can probably stem from the Ag NP ethanol/water solution whose slow aggregation has been evidenced by UV–vis absorption spectra already (figure 2, curve (b)).

3.4. Effect of deposition technique on Ag NP arrangement

With respect to the results discussed in section 3.3, Ag NPs dispersed in the ethanol/water (1/1, v/v) mixture were chosen for our further experiments. However, a drop-casting strategy was applied instead of the dip-coating of the substrates in the diluted Ag NP solutions. Simply, small drops of the Ag NP solution were deposited and then allowed to dry on the cold plasma-treated and -untreated substrates. Without doubt, the observed processes as well as results differed on the plasma-treated and -untreated substrates. The drops deposited on the cold plasma-treated substrate spread quickly (figure 4(B)), while those on the untreated substrate did not (figure 4(A)). This observation unequivocally confirmed that the cold plasma treatment of the substrates increased their hydrophilicity. Apparently, rings consisting of 3D aggregates of Ag NPs (figure 4(C) and appropriate detail) resulted from the evaporation of drops deposited on the untreated substrates. In contrast, 2D self-assemblies of Ag NPs were formed in the case of the plasma-treated substrates (figure 4(D) and appropriate detail). It can thus be concluded that the choice of a suitable Ag concentration, solvent mixture, volume and spacing of drops which will be deposited by the drop-casting technique on the cold plasma-treated substrates can lead to a regular coverage of the substrate surface by 2D self-assembled Ag NPs.

In figure 5, the SEM images of the untreated and plasma-treated substrates modified by Ag NPs are compared when the optimal deposition conditions were reached. These samples have been further investigated by XPS and UPS measurements

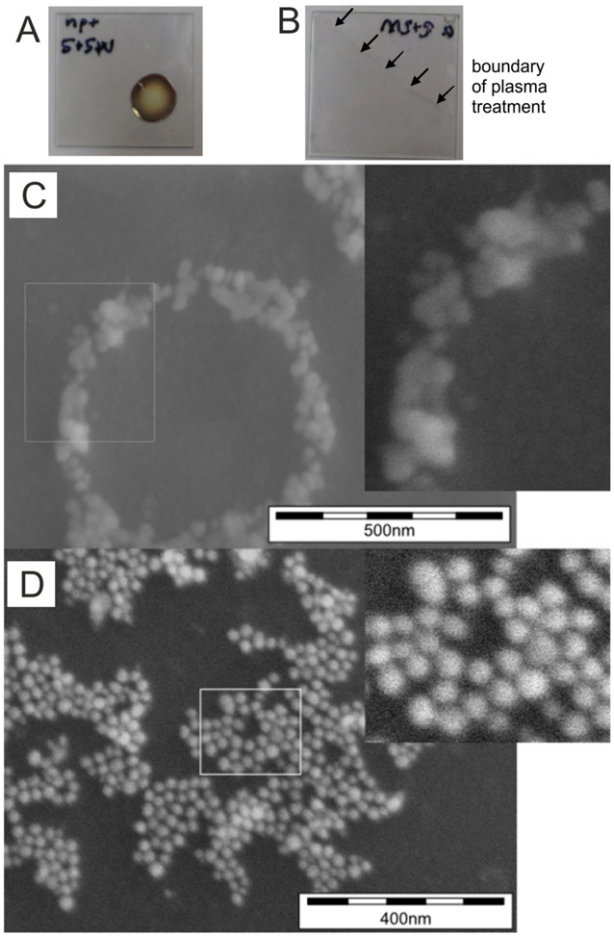

Figure 4. Photography of (A) plasma-untreated and (B) plasma-treated ITO-coated glass with a deposited drop of Ag NP dispersion. SEM images of (C) untreated and (D) cold plasma-treated ITO substrates covered with Ag NPs which were deposited by a 10 μl drop of the diluted Ag NPs ethanol/water (1/1, v/v) solution. Details demonstrate the 3D and 2D arrangement of Ag NPs.

(the results of the latter technique will be discussed in section 3.5). According to the XPS analysis of Ag 3d peaks, a higher relative content of Ag has been determined for the 3D (0.48 at.%) than for 2D (0.23 at.%) self-assembled Ag NPs (figure 6). This implicitly confirms the dimensionality of self-assembling, i.e. one layer of Ag NPs for the 2D self-assembly and more than two layers for the 3D self-assembly.

3.5. Work functions of Ag NP-unmodified and-modified ITO-coated substrates

The DCSBD generator used in our study provides a spatially homogeneous plasma. Since the depth of the cold plasma effect goes only into the tenths of one micrometer [14], the cold plasma treatment of substrates can be called a nano-modification of their surfaces. A very important fact is that the nano-modification does not change the electrical properties of ITO coatings. We have checked the values of the work function of ITO-coated substrates by means of UPS measurements. The value of the work function for cleaned bare ITO substrates was 4.61 eV, while that of the cold plasma-treated ITO substrates

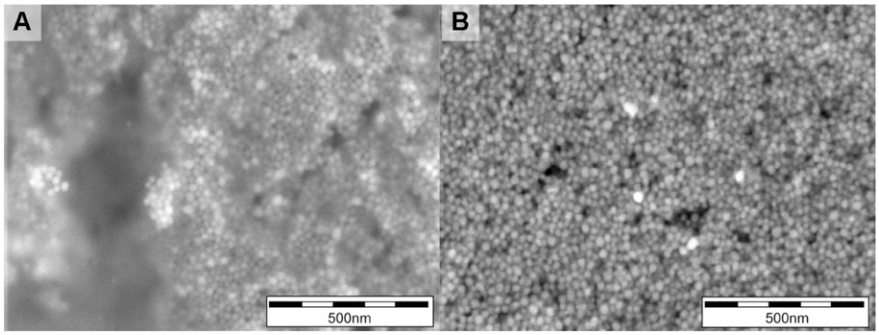

Figure 5. SEM images of (A) plasma-untreated and (B) cold plasma-treated ITO-coated substrates fully covered by Ag NPs which were deposited by the drop-casting technique of the diluted Ag NP ethanol/water (1/1, v/v) solution.

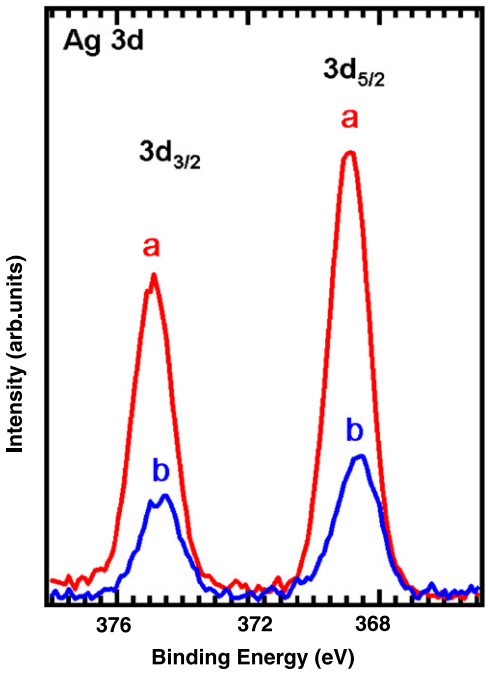

Figure 6. XPS analysis of Ag 3d peaks performed on (a) plasma-untreated ITO-coated substrates modified by 3D arrangement of Ag NPs, (b) cold plasma-treated ITO-coated substrates modified by 2D self-assembled Ag NPs.

Table 3. Work functions of Ag NP-modified and -unmodified ITO-coated substrates determined by UPS.

Sample	Work function (eV)
Bare ITO	4.61
Plasma-treated ITO	4.64
Ag NPs on bare ITO	3.64
Ag NPs on plasma-treated ITO	4.38

was 4.64 eV (table 3). The difference of 0.03 eV is within the experimental error.

As has already been pinpointed in section 1, the work function is the crucial characteristic of electrodes (i.e. conductive substrates) applied in opto-electronic devices [26–28]. According to the literature, the work function of electrodes can change owing to the cleaning method [32] or due to self-assembled monolayers of organic molecules [33–36]. We have modified ITO electrodes by Ag NPs and measured their work function (table 3). The results clearly show that the 3D aggregates of Ag NPs on ITO-coated glass, observed in figure 5(A), provide a lower value of the work function (3.64 eV) than the bare ITO-coated substrate, while the 2D self-assemblies of Ag NPs, visualized in figure 5(B), give a value of 4.38 eV. The latter is virtually the same value as that of bulk Ag (4.4 eV) [34]. The same result, i.e. the work function of bulk Ag, has been obtained for the plasma pre-treated piece of glass modified by Ag NP 2D self-assemblies. This is quite encouraging taking into account that the formation of our 2D self-assemblies of Ag NPs on the substrates is very easy and possibly applicable on a large scale (when the optimal conditions are met).

Moreover, the dried 2D self-assemblies of Ag NPs are resistant to washing with non-polar organic solvents such as chloroform and/or toluene. In particular, this result is very important and useful for the further applications of the Ag NP-modified plasma pre-treated substrates in OSC and/or OLED devices because the next layer consists of a conductive polymer which is usually deposited from a non-polar solvent (and/or non-polar solvent mixture).

Last, but not least, it should be pointed out that the 2D self-assemblies of any NPs dispersed in a suitable polar solvent mixture may be formed on any other substrate which is going to replace ITO-coated substrates and which is treated by the cold plasma under ambient conditions prior to the NPs' deposition.

4. Conclusions

Cold plasma treatment of selected substrates (particularly, glass and indium–tin-oxide coated substrates) has been successfully exploited for the formation of spontaneous 2D self-assemblies of Ag NPs on the substrate surface. Moreover, the work function, a substantial characteristic of conductive surfaces, has been determined for the Ag NP-modified substrates by means of ultraviolet photoelectron spectroscopy. In our experiments, we have focused on several parameters influencing the final coverage of plasma-treated substrates by Ag NPs such as (i) the deposition technique, (ii) Ag NP concentration, and (iii) the solvent mixture where Ag NPs were dispersed. The possibility of an easy modification of substrates

by 2D self-assemblies of Ag NPs at room temperature and atmospheric pressure without using any chemical treatment and/or evaporation chamber is an important advantage of the brand new applications of diffuse coplanar surface barrier discharges.

Acknowledgments

The authors thank Ivo Medřík for his technical help with the DCSBD generator and Dr Jana Soukupová for the preparation of the Ag NPs stock-solution. Dr Šišková thanks the Fulbright foundation which enabled her to meet Dr Seo and to learn many details about the preparation of OSC and OLED devices in the USA, at UCSB. The financial support by KAN101630651 and KAN115600801 research projects is gratefully acknowledged.

References

[1] Rotello V (ed) 2004 *Nanoparticle Building Blocks for Nanotechnology* (New York: Kluwer Academic) chapter 7 (Plasmonic Nanomaterials)
[2] Sharma V, Yngard R A and Lin Y 2009 *Adv. Colloid Interface Sci.* **145** 83
[3] Park H J, Vak D, Noh Y Y, Lim B and Kim D Y 2007 *Appl. Phys. Lett.* **90** 161107
[4] Morfa A, Rowlen K L, Reilly T H III, Romero M J and van de Lagemaat J 2008 *Appl. Phys. Lett.* **92** 013504
[5] Kim S S, Na S I, Jo J, Kim D Y and Nah Y Ch 2008 *Appl. Phys. Lett.* **93** 073307
[6] Lee J H, Park J H, Kim J S, Lee D Y and Cho K 2009 *Org. Electron.* **10** 416
[7] Juillerat F, Solak H H, Bowen P and Hofmann H 2005 *Nanotechnology* **16** 1311
[8] Yao H, Yi Ch, Tzang Ch-H, Zhu J and Yang M 2007 *Nanotechnology* **18** 015102
[9] Chen X Y, Li J R, Jiang L, Chen X Y and Li J R 2000 *Nanotechnology* **11** 108
[10] Grzelczak M, Vermant J, Furst E M and Liz-Marzan L M 2010 *ACS Nano* **4** 3591
[11] Ishii M, Mori T, Fujikawa H, Tokito S and Taga Y 2000 *J. Lumin.* **87–89** 1165
[12] Chan I M, Cheng W Ch and Hong F C 2002 *Appl. Phys. Lett.* **80** 13–15
[13] Hippler R, Kersten H, Schmidt M and Schoenbach K H (ed) 2008 *Low Temperature Plasmas: Fundamentals, Technologies, and Techniques* vol 2 (Weinheim: Wiley–VCH)
[14] Kogelschatz U 2003 *Plasma Chem. Plasma Process.* **23** 1
[15] Borcia G, Anderson C A and Brown N M D 2004 *Appl. Surf. Sci.* **221** 203
[16] Borcia G, Anderson C A and Brown N M D 2004 *Appl. Surf. Sci.* **225** 186
[17] Kim S H, Cho S H, Lee N E, Kim H M, Nam Y W and Kim Y H 2005 *Surf. Coat. Technol.* **193** 101
[18] Hoecker H 2002 *Pure Appl. Chem.* **74** 423
[19] De Geyter N, Morent R and Leys C 2006 *Surf. Coat. Technol.* **201** 2460
[20] Borcia G, Anderson C A and Brown N M D 2006 *Surf. Coat. Technol.* **201** 3074
[21] Steen M L, Hymas L, Havey E D, Capps N E, Castner D G and Fisher E R 2001 *J. Membr. Sci.* **188** 97
[22] Kodama S, Habaki H, Sekiguchi H and Kawasaki J 2002 *Thin Solid Films* **407** 151
[23] Major S, Kumar S, Bhatnagar M and Chopra K L 1986 *Appl. Phys. Lett.* **49** 394
[24] Wu C C, Wu C I, Sturm J C and Kahn A 1997 *Appl. Phys. Lett.* **70** 1348
[25] Wang Ch and He X 2006 *Appl. Surf. Sci.* **253** 926
[26] Chen C P, Tien T C, Ko B T, Chen Y D and Ting C 2009 *ACS Appl. Mater. Interfaces* **1** 741
[27] Braun S, Salaneck W R and Fahlman M 2009 *Adv. Mater.* **21** 1450
[28] Frohne H, Shaheen S E, Brabec C J, Muller D C, Sariciftci N S and Meerholz K 2002 *Chem. Phys. Chem.* **9** 795
[29] Kvitek L, Prucek R, Panacek A, Novotny R, Hrbac J and Zboril R 2005 *J. Mater. Chem.* **15** 1099
[30] *IUPAC Compendium of Chemical Terminology* 1997 2nd edn (Cambridge: RSC)
[31] Rabani E, Reichman D R, Geissler P L and Brus L E 2003 *Nature* **426** 271
[32] Sugiyama K, Ishii H, Ouchi Y and Seki K 2000 *J. Appl. Phys.* **87** 295
[33] Carrara M, Kakkassery J J, Abid J P and Fermin D J 2004 *Chem. Phys. Chem.* **5** 571
[34] de Boer B, Hadipour A, Mandoc M M, van Woudenbergh T and Blom P W M 2005 *Adv. Mater.* **17** 621
[35] Schnippering M, Carrara M, Foelske A, Kotz R and Fermin D J 2007 *Phys. Chem. Chem. Phys.* **9** 725
[36] Wu K Y, Yu S Y and Tao Y T 2009 *Langmuir* **25** 6232